NASA TN D-1456

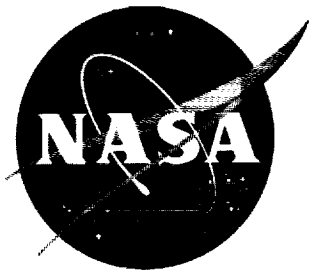

TECHNICAL NOTE

D-1456

OPTIMUM LOW-ACCELERATION TRAJECTORIES FOR INTERPLANETARY TRANSFERS

By Arthur V. Zimmerman, John S. MacKay,
and Leonard G. Rossa

Lewis Research Center
Cleveland, Ohio

NATIONAL AERONAUTICS AND SPACE ADMINISTRATION

WASHINGTON January 1963

NATIONAL AERONAUTICS AND SPACE ADMINISTRATION

TECHNICAL NOTE D-1456

OPTIMUM LOW-ACCELERATION TRAJECTORIES FOR INTERPLANETARY TRANSFERS

By Arthur V. Zimmerman, John S. MacKay,
and Leonard G. Rossa

SUMMARY

The methods of the calculus of variations are used to find functions of time for the thrust magnitude and direction that minimize the propellant consumption for a given interplanetary transfer. The flight is assumed to be planar and to take place in an inverse-square gravitational field. Propulsion is provided by a fixed thrust and specific impulse engine that can be turned on and off at will. With such an engine, the determination of the thrust-magnitude function reduces to finding the best points at which to begin and end a coast phase.

Numerical results are presented for one-way trips from Earth to Mars and from Mars to Earth (both assumed in coplanar, circular orbits) for three values of initial acceleration (0.5×10^{-4}, 1×10^{-4}, and 5×10^{-4} Earth standard g's) and five values of specific impulse (2000, 4000, 6000, 8000, and 10,000 sec). For these engine parameters, the trip time is varied between the continuous-propulsion time and the optimum time, which is analogous to the two-impulse, Hohmann transfer for impulsive thrust. These results are compared with the constant-jet-power, variable-thrust engine for the case of transfers to the best point on the Martian ellipse.

Although the variational solution for round trips is not considered, the one-way trip data of the type presented may be used to calculate equivalent results. A sample calculation is given to illustrate the procedure.

INTRODUCTION

The long propulsion periods associated with low-acceleration flight give rise to the problem of determining appropriate functions of time for engine thrust magnitude and direction in order to minimize the propellant consumed in accomplishing a given mission. As shown in references 1 to 4, such functions can be found by use of the indirect methods of the calculus of variations. In formulating such a problem it is necessary to introduce constraints

on the engine thrust and specific impulse consistent with the assumed mode of engine operation. Otherwise, as shown in reference 1, the variational solution will yield infinite thrust and specific impulse. The purpose of this report is to present a variational solution with constraints specifically designed for early ion engines. This solution is then used to determine optimum trajectories for both the outbound and inbound heliocentric portions of low-thrust Mars missions. The resulting variational solution can also be applied to many other trajectory problems or to flight with chemical- and nuclear-rocket engines operating under similar contraints.

In references 2 and 5 the thrust and specific impulse for ion engines were limited by constraining engine operation to constant beam power; the resulting solution required large variations in thrust and specific impulse along the path. Early ion engines probably will be capable of operating efficiently over only limited ranges of thrust and specific impulse. Thus, although the variable-thrust trajectories of references 2 and 5 represent an upper bound on the capabilities of future ion engines, they are not applicable to early ion engines. The contraints assumed in the present analysis are that engine thrust and specific impulse (and, hence, beam power) are constant. Since it is assumed that the engines are capable of shutdown and restart, the trajectories may have coast phases. This problem is treated in reference 3 for the case of a constant planar gravitational field. Reference 5 presents a more comprehensive solution that includes a spherical inverse-square gravitational field and covers both the constant-thrust and variable-thrust cases. The solution of the present report is specifically for the constant-thrust case in a two-dimensional inverse-square gravitational field and contains more detailed and extensive information about this case than has been presented elsewhere. Emphasis is placed herein on a discussion of the nature of the optimizations and the effect of initial thrust-to-weight ratio and specific impulse. Furthermore, typical results are given to illustrate the analysis of round-trip missions.

The variational analysis results in a set of Euler-Lagrange differential equations that yield the optimum thrust direction and indicate the best times for initiating and terminating the coast phase. Numerical results were obtained by simultaneous numerical integration of the Euler-Lagrange equations with the equations of motion on an IBM 704 digital computer. As shown in reference 4, all the differential equations can be analytically integrated during the coast phase. The analytical solutions to the Euler-Lagrange equations for the present problem are presented in appendix B. The details of all numerical techniques employed here are given in reference 6.

Sufficient numerical data are presented to indicate the nature of constant-thrust trajectories and to allow computation of some specific one-way and round-trip missions. Charts are presented for both Earth-Mars and Mars-Earth transfers that use an optimum travel angle. The data are presented as a function of

travel time and specific impulse for thrust-to-weight ratios of 0.5×10^{-4}, 1×10^{-4}, and 5×10^{-4}. The constant-thrust transfers are briefly compared with the variable-thrust transfers presented in reference 2.

For round-trip missions, nonoptimum travel angles will generally be required to meet planetary configurations. Thus, data for a wide range of travel angles are presented for a few representative values of thrust-to-weight ratio and specific impulse. These data are then used to illustrate a round-trip calculation.

ANALYSIS

The problem to be solved is to determine the vehicle thrust program and hence the trajectory that minimizes the amount of propellant consumed in accomplishing a given mission. The engine is assumed to operate at constant thrust and specific impulse during powered flight, but it can be turned off for coast flight. For simplicity the vehicle is assumed to move in a two-dimensional trajectory in a central inverse-square gravitational field.

The vehicle trajectory must satisfy the following equations of motion:

$$\dot{u} = -\frac{\mu}{r^2} + \omega^2 r + \frac{V_j \beta}{m} \sin \psi \tag{1a}$$

$$\dot{\omega} = -\frac{2u\omega}{r} + \frac{V_j \beta}{m} \frac{\cos \psi}{r} \tag{1b}$$

$$\dot{r} = u \tag{1c}$$

$$\dot{\phi} = \omega \tag{1d}$$

where

$$\dot{m} = -\beta \tag{1e}$$

(All symbols are defined in appendix A.) In order to satisfy the engine constraints, the exhaust velocity V_j is treated as a constant throughout the flight, and the propellant flow rate β is given by

$$\left.\begin{aligned} \beta &= \beta_{des} = \text{const} \quad && \text{for powered flight} \\ \beta &= 0 && \text{for coast flight} \end{aligned}\right\} \tag{2}$$

Formulation of Variational Problem

The variational problem to be solved is to determine ψ and β as functions of time, subject to the constraints given by equations (1) and (2), so that the amount of propellant consumed in accomplishing a given mission is minimized. This problem is a special case of the problem of Bolza as formulated in reference 7 and is known in the calculus of variations as the problem of Mayer. The Multiplier Rule and associated corollaries developed in reference 7 will be used to solve this problem. In the problem of Mayer a function g of the initial and final conditions is minimized. To minimize the propellant consumption (or equivalently, the negative of final mass), g is given by

$$g = -m_f \tag{3}$$

The constraints given by equations (1) and (2) are introduced through the function F defined by

$$F = \sum_{i=1}^{6} f_i \lambda_i \tag{4}$$

where

$$f_1 = \dot{u} + \frac{\mu}{r^2} - \omega^2 r - \frac{V_j \beta}{m} \sin \psi = 0 \tag{5a}$$

$$f_2 = r\dot{\omega} + 2u\omega - \frac{V_j \beta}{m} \cos \psi = 0 \tag{5b}$$

$$f_3 = \dot{r} - u = 0 \tag{5c}$$

$$f_4 = \dot{\varphi} - \omega = 0 \tag{5d}$$

$$f_5 = \dot{m} + \beta = 0 \tag{5e}$$

$$f_6 = \beta(\beta - \beta_{des}) = 0 \tag{5f}$$

and the λ_i (where $i = 1, 2, \ldots, 6$) are the Lagrangian multipliers, which are unknown functions of time to be determined as part of the variational solution.

Equations (5a) to (5d) are the equations of motion (eqs. (1a) to (1e)). Equation (5e) is the differential equation for the vehicle mass. Equation (5f) states the constraints on the propellant flow rate β given by equation (2); namely, that the propellant flow rate must be zero or the design value. At this

point it is convenient to introduce the following notation for the dependent variables of the problem:

$$Z_1(t) = u \qquad Z_5(t) = m$$

$$Z_2(t) = \omega \qquad Z_6(t) = \psi$$

$$Z_3(t) = r \qquad Z_7(t) = \beta$$

$$Z_4(t) = \varphi$$

Euler-Lagrange Equations

As developed in reference 7, a necessary condition for g to be a minimum is that the Euler-Lagrange equation with respect to each dependent variable be satisfied. The Euler-Lagrange equations are given by

$$\frac{d}{dt}\left(\frac{\partial F}{\partial \dot{Z}_i}\right) = \frac{\partial F}{\partial Z_i} \qquad i = 1, 2, \ldots, 7 \tag{6}$$

Applying equation (6) to equation (4) results in the Euler-Lagrange equations for the present problem:

$$\dot{\lambda}_1 = 2\omega\lambda_2 - \lambda_3 \tag{7a}$$

$$\dot{\lambda}_2 = -2\omega\lambda_1 + \frac{u}{r}\lambda_2 - \frac{\lambda_4}{r} \tag{7b}$$

$$\dot{\lambda}_3 = -\left(\frac{2\mu}{r^3} + \omega^2\right)\lambda_1 + \dot{\omega}\lambda_2 \tag{7c}$$

$$\dot{\lambda}_4 = 0 \tag{7d}$$

$$\dot{\lambda}_5 = \frac{V_j\beta}{m^2}(\lambda_1 \sin\psi + \lambda_2 \cos\psi) \tag{7e}$$

$$(\lambda_1 \cos\psi - \lambda_2 \sin\psi)\frac{V_j\beta}{m} = 0 \tag{7f}$$

$$\lambda_6 = \frac{\frac{V_j}{m}(\lambda_1 \sin\psi + \lambda_2 \cos\psi) - \lambda_5}{2\beta - \beta_{des}} \tag{7g}$$

The differential equations (7a) to (7e) must be integrated along with the equations of motion (eqs. (1a) to (1e)) to determine the optimum trajectory. Equation (7g) serves only to define λ_6 and has no further significance in the

present problem. Equation (7f) gives the value of the thrust angle along the optimum trajectory during powered flight (The value of the thrust angle is not required during coast flight). From equation (7f):

$$\tan \psi = \frac{\lambda_1}{\lambda_2} \qquad \text{for} \quad \beta = \beta_{des} \tag{8}$$

or

$$\sin \psi = \frac{\lambda_1}{\pm\sqrt{\lambda_1^2 + \lambda_2^2}} \tag{9a}$$

$$\cos \psi = \frac{\lambda_2}{\pm\sqrt{\lambda_1^2 + \lambda_2^2}} \tag{9b}$$

The uncertainty in the signs of equations (9a) and (9b) corresponds to an uncertainty of π in the value of the thrust angle ψ (i.e., ψ or $\psi + \pi$). The choice of sign for equations (9a) and (9b) is developed later in the section Necessary Condition of Weierstrass. Integrating equation (7d) gives

$$\lambda_4 = \text{const} \tag{10}$$

Another integral of the Euler-Lagrange equations can be obtained, since the function F does not contain the independent variable, time, explicitly. From reference 7,

$$F - \sum_{i=1}^{7} \dot{Z}_i \frac{\partial F}{\partial \dot{Z}_i} = \int_0^{t_f} \frac{\partial F}{\partial t}\, dt + C \tag{11}$$

In the present case, where the function F does not contain time explicitly, this reduces to

$$F - \sum_{i=1}^{7} \dot{Z}_i \frac{\partial F}{\partial \dot{Z}_i} = C \tag{12}$$

or from equations (4) to (5f)

$$\left(\frac{\mu}{r^2} - \omega^2 r - \frac{V_j \beta}{m} \sin \psi\right)\lambda_1 + \left(2u\omega - \frac{V_j \beta}{m} \cos \psi\right)\lambda_2 - u\lambda_3 - \omega\lambda_4 + \beta\lambda_5 = C \tag{13}$$

Equation (13) can be used to determine the value of one of the Lagrangian multipliers. In the present case it is convenient to determine λ_5 from equation (13) and eliminate the need for integrating equation (7e). Thus,

$$\lambda_5 = \frac{C - \left(\frac{\mu}{r^2} - \omega^2 r - \frac{V_j \beta}{m} \sin \psi\right) \lambda_1 - \left(2u\omega - \frac{V_j \beta}{m} \cos \psi\right) \lambda_2 + u\lambda_3 + \omega\lambda_4}{\beta}$$

$$\text{for} \quad \beta \neq 0 \qquad (14)$$

To evaluate λ_5 for $\beta = 0$, it should be noted from equation (7e) that in this case $\dot{\lambda}_5 = 0$. Thus, λ_5 is a constant during coast. Specifically, λ_5 is equal to its value at the termination of the previous propulsive phase of the trajectory. The continuity of λ_5 at the point of transition from powered flight to coast is established by applying the Weierstrass-Erdmann Corner Condition (ref. 7). This condition states that the $\partial F/\partial \dot{Z}_i$ must have equal right- and left-hand limits at such corners. For the present problem

$$\frac{\partial F}{\partial \dot{u}} = \lambda_1 \qquad \frac{\partial F}{\partial \dot{m}} = \lambda_5$$

$$\frac{\partial F}{\partial \dot{\omega}} = r\lambda_2 \qquad \frac{\partial F}{\partial \dot{\psi}} = 0$$

$$\frac{\partial F}{\partial \dot{r}} = \lambda_3 \qquad \frac{\partial F}{\partial \dot{\beta}} = 0$$

$$\frac{\partial F}{\partial \dot{\varphi}} = \lambda_4$$

Therefore, at a corner such as the transition from powered flight to coast (and vice versa), the Lagrangian multipliers λ_1 to λ_5 have equal right- and left-hand limits. This implies that the constant of integration C is also continuous at the corners.

Necessary Condition of Weierstrass

Two uncertainties still remain in the system of Euler-Lagrange equations. The first is the choice of signs in equations (9a) and (9b), and the second is the value of β (i.e., $\beta = \beta_{des}$ or 0) along the path. Both of these uncertainties are resolved by applying the Necessary Condition of Weierstrass (ref. 7). Following the development in reference 3, this condition states that for a minimizing trajectory $E \geq 0$ where

$$E = F\left(Z_i^*, \dot{Z}_i^*\right) - F\left(Z_i, \dot{Z}_i\right) - \sum_{i=1}^{7} \left(\dot{Z}_i^* - \dot{Z}_i\right) \frac{\partial F}{\partial \dot{Z}_i} \geq 0 \tag{15}$$

The Z_i's are the actual minimizing functions, and the Z_i^*'s denote functions differing from the Z_i's by finite, admissible amounts. In the present problem only ψ and β are subject to such strong variations. Equation (15) may then be written as

$$\beta\left[\frac{V_j}{m}\left(\lambda_1 \sin\psi + \lambda_2 \cos\psi\right) - \lambda_5\right] - \beta^*\left[\frac{V_j}{m}\left(\lambda_1 \sin\psi^* + \lambda_2 \cos\psi^*\right) - \lambda_5\right] \geq 0 \tag{16}$$

In the notation of reference 3, let

$$k = \frac{V_j}{m}\left(\lambda_1 \sin\psi + \lambda_2 \cos\psi\right) - \lambda_5 \tag{17a}$$

$$k^* = \frac{V_j}{m}\left(\lambda_1 \sin\psi^* + \lambda_2 \cos\psi^*\right) - \lambda_5 \tag{17b}$$

Then

$$\beta k - \beta^* k^* \geq 0 \tag{18}$$

Inequality (18) is now examined for the admissible variations in ψ and β.

$\underline{\beta = \beta^* = \beta_{des},\ \psi \neq \psi^*}$. - In this case inequality (18) reduces to

$$k - k^* \geq 0 \tag{19}$$

or

$$\lambda_1 \sin\psi + \lambda_2 \cos\psi \geq \lambda_1 \sin\psi^* + \lambda_2 \cos\psi^* \tag{20}$$

Since, for any value of ψ, ψ^* can only equal $\psi + \pi$,

$$\lambda_1 \sin\psi + \lambda_2 \cos\psi \geq 0 \tag{21}$$

Substituting equations (9a) and (9b) in inequality (21) results in

$$\pm\sqrt{\lambda_1^2 + \lambda_2^2} \geq 0 \tag{22}$$

Therefore, the plus sign is used in equations (9a) and (9b).

$k = k^*$, $\beta \neq \beta^*$. - In this case inequality (18) reduces to

$$k(\beta - \beta^*) \geq 0 \tag{23}$$

When k is negative, β must be less than β^* and thus β is zero. Similarly, when k is positive, β must be greater than β^* and thus β equals β_{des}. In summary,

$$\begin{aligned} \beta &= \beta_{des} \qquad \text{for} \quad k \geq 0 \\ \beta &= 0 \qquad\quad\ \ \text{for} \quad k \leq 0 \end{aligned} \tag{24}$$

The sign of k then determines the powered and coast phases of the flight, and the transition from one phase to another occurs at $k = 0$.

The variational equations developed thus far are independent of the function g; this is characteristic of the problem of Mayer, in which g is only a function of the initial and final conditions. The specific nature of g influences only the boundary conditions that must be satisfied in integrating the equations of motion and the Euler-Lagrange equations.

Boundary Conditions

If some of the Z_i's are not specified at either end of the trajectory, the free boundary values should be selected to minimize g. The boundary conditions that must be satisfied for the minimizing trajectory are given by the transversality condition (ref. 7). This condition states that for a minimizing trajectory

$$\left[\left(F - \sum_{i=1}^{7} \dot{Z}_i \frac{\partial F}{\partial \dot{Z}_i}\right) dt + \sum_{i=1}^{7} \frac{\partial F}{\partial \dot{Z}_i} dZ_i\right]_0^f + dg = 0 \tag{25}$$

By use of equations (4), (5a) to (5f), and (12), equation (25) becomes

$$C\ dt + \lambda_1\ du + r\lambda_2\ d\omega + \lambda_3\ dr + \lambda_4\ d\varphi + \lambda_5\ dm \Big|_0^f + dg = 0 \tag{26}$$

Further evaluation of the boundary conditions to be satisfied requires application of equation (26) to a specific problem. In this analysis the problem of minimizing the propellant consumed in transferring between circular, coplanar orbits is examined. (The problem of transfer between elliptic orbits is discussed in appendix C). For this case g is given by equation (3), and the following initial and final boundary conditions are known:

Initial	Final
m_0	r_f
r_0	$\omega_f = \sqrt{\mu/r_f^3}$
$\omega_0 = \sqrt{\mu/r_0^3}$	$u_f = 0$
$u_0 = 0$	
$\varphi_0 = 0$	
$t_0 = 0$	

(27)

The final time t_f and angle φ_f may be specified or left free for further optimization of the final mass. As a consequence of the aforementioned boundary conditions (eqs. (27)),

$$dm_0 = dr_0 = d\omega_0 = du_0 = d\varphi_0 = dt_0 = dr_f = d\omega_f = du_f = 0 \tag{28}$$

and equation (26) reduces to

$$C\ dt_f + \lambda_4\ d\varphi_f + (\lambda_{5,f} - 1)\ dm_f = 0 \tag{29}$$

where the variations dt_f, $d\varphi_f$, and dm_f are independent. If t_f, φ_f, and m_f are not specified, their variations in equation (29) are nonzero and their respective coefficients must be zero.

Since m_f is the quantity subject to optimization, it is not specified and $dm_f \neq 0$. Thus, equation (29) gives as one boundary condition to be satisfied:

$$\lambda_{5,f} = 1 \tag{30}$$

If the position in the final circular orbit is not specified $d\varphi_f \neq 0$, and equation (29) gives

$$\lambda_4 = 0 \tag{31}$$

Thus, a circular-orbit transfer with $\lambda_4 = 0$ yields the trajectory possessing the optimum travel angle. If the final time is not specified $dt_f \neq 0$, and equation (29) also gives

$$C = 0 \tag{32}$$

Thus, a circular-orbit transfer with $C = 0$ yields the trajectory having the optimum travel time.

Calculation Procedure and Two-Point Boundary Value Problem

The equations required for the determination of the minimizing trajectory are summarized for convenience in appendix D. The equations of motion (eqs. (1a) to (1e)) and the Euler-Lagrange equations (eqs. (7a) to (7c)) must be integrated simultaneously to determine the minimizing trajectory. The value of the thrust angle is given by equations (9a) and (9b), and the powered and coast phases are indicated by equation (24). These equations were programed for an IBM 704 computer and integrated numerically with a Runge-Kutta technique by use of a step-size control to limit the truncation error.

For the problem of transferring between circular orbits the known initial conditions were given by equations (27). In order to proceed with the trajectory integration, values for the $\lambda_i(0)$ must also be chosen. The values for the $\lambda_i(0)$ must be selected to satisfy the desired final conditions given by equations (27) and those obtained from the transversality condition (eq. (29)); this results in what is commonly known as a two-point boundary value problem. Specifically,

Unknown initial conditions	Desired final conditions
$\lambda_1(0)$	$r(t_f)$
$\lambda_2(0)$	$u(t_f) = 0$
$\lambda_3(0)$	$\omega(t_f) = \sqrt{\mu/r_f^3}$
$\lambda_4 = \text{const}$	$\varphi(t_f)$
C	t_f
	$\lambda_{5,f} = 1.0$

(33)

where for convenience C is selected as an initial condition to be determined rather than λ_5.

To simplify the set of conditions (33), first note that the Euler-Lagrange equations (eqs. (7a) to (7g)) are homogeneous in λ_i. This means that the solution is independent of the initial magnitude of one of the λ_i's, which can be considered to act as only a scale factor for the other λ_i's. In the present case, $\lambda_3(0)$ was selected as the scale factor, and its initial magnitude was taken as unity. After a solution is obtained, the requirement $\lambda_{5,f} = 1$ can

then be satisfied by merely adjusting the scale factor $\lambda_3(0)$. Thus $\lambda_3(0)$ and $\lambda_{5,f} = 1$ can be removed from the iteration.

A further simplification was made in the present analysis by not specifying φ_f; hence, λ_4 was removed from the iteration. The solutions for optimum φ_f were obtained with $\lambda_4 = 0$, and the solution for nonoptimum φ_f were obtained by covering a range in λ_4. Finally, the desired t_f is obtained by terminating the trajectory integration at $t = t_f$. The set of boundary conditions (33) then becomes the following:

Unknown initial conditions	Desired final conditions
$\lambda_1(0)$	$r(t_f) = r_f$
$\lambda_2(0)$	$u(t_f) = 0$
C	$\omega(t_f) = \sqrt{\mu/r_f^3}$

(34)

Obtaining a solution, then, requires that the values of three initial conditions be determined such that the three specified final conditions are satisfied. This problem was solved by use of a three-variable Newton-Raphson iteration scheme wherein the various required partial derivatives were evaluated by finite-difference methods. The iterations were terminated when residual errors in the end conditions were such that their removal would cost no more than a specified amount of propellant. The iteration scheme, as well as the criterion for terminating the iteration, is discussed in reference 6.

RESULTS AND DISCUSSION

The variational solution developed in the ANALYSIS has been used to investigate the heliocentric phases of Earth-Mars and Mars-Earth low-thrust transfer trajectories. In making preliminary analyses of low-thrust interplanetary missions, it is convenient to assume a series of two-body trajectories rather than treating the precise multibody problem (ref. 8). For example, for the Earth-Mars mission, the Earth escape spiral can be computed from consideration of Earth's gravitational field only. When the vehicle has traveled a sufficient distance from the Earth, the coordinates can be transferred to the sun; and during heliocentric flight, only the solar gravitational field can be considered. Again, when the vehicle has approached sufficiently close to Mars, the coordinates can be transferred to Mars; and during the descent spiral, only the Martian gravitational field is considered.

The variational solution developed in the ANALYSIS can be applied to all three phases of such a journey. Only the heliocentric portion, however, has been investigated herein. Data for the Earth escape and Mars descent spirals can be obtained from the charts of reference 8, which are based on a constant-tangential-thrust steering program. For constant-thrust spirals, this steering program has been shown to give near optimum results (ref. 2).

Boundary Conditions

The boundary conditions imposed on the heliocentric trajectories presented in this report are based on transfer from geocentric to heliocentric coordinates when the vehicle has achieved escape energy with respect to the Earth and transfer from heliocentric to Martian coordinates when the vehicle is at escape energy with respect to Mars. Thus, the heliocentric trajectories begin with the vehicle in Earth's orbit about the sun and terminate with the vehicle in Mars' orbit about the sun. For simplicity, Earth and Mars are assumed to move in circular, coplanar orbits about the sun. Assuming a circular orbit for Mars can lead to significant errors in some cases. An elliptic orbit for Mars is treated in appendix C. The values in the following table were used for the orbits of Earth and Mars:

Planet	Radius, r, m	Polar angular velocity, ω, radians/sec
Earth	1.4950×10^{11}	1.9910×10^{-7}
Mars	2.2779×10^{11}	1.0586×10^{-7}

These values are based on a solar gravitational constant $\mu = 1.3245 \times 10^{20}$ m^3/sec^2. The boundary conditions are satisfied to the extent that the residual errors result in an error in final mass of less than 0.1 percent of m_0.

Earth-Mars Transfers

The transfer trajectories investigated herein are limited to direct transfers making less than 1 revolution about the sun. The resulting flights, in general, have either continuous propulsion or two propulsive phases with an intermediate coast phase. To indicate the nature of these transfers, the Earth-Mars transfers will be examined in detail for one set of engine parameters. Similar results would be obtained for Mars-Earth transfers. The reference set of engine parameters selected is an initial thrust-to-weight ratio of 1×10^{-4} and a specific impulse of 8000 seconds. Later, data for both Earth-Mars and Mars-Earth transfers for a range of engine parameters are presented.

Effect of travel time. - The effect of travel time on Earth-Mars transfer trajectories for the reference engine parameters is illustrated graphically in figure 1(a). The flights shown have an optimum travel angle (corresponding to $\lambda_4 = 0$). The quickest transfer, 181.6 days, is obtained with continuous propulsion. As travel time is increased, the length of the coast phase increases; and at approximately 290 days, the trip having the optimum travel time (corresponding to $C = 0$) is obtained. This journey is analogous to the Hohmann transfer for impulsive thrust and has the longest intermediate coast phase.

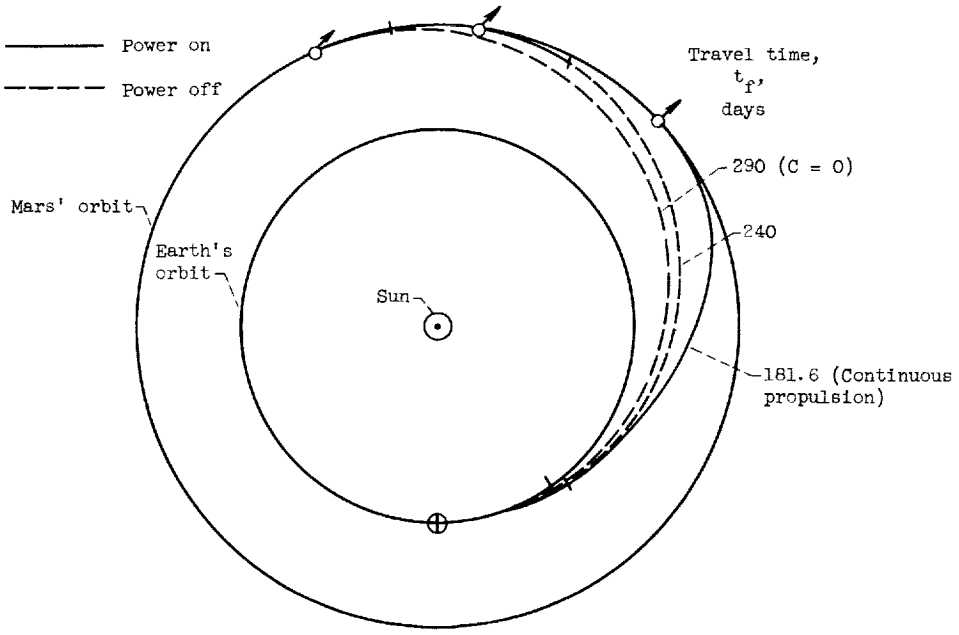

(a) Trajectory profiles.

Figure 1. - Effect of travel time on Earth-Mars transfers. Initial thrust-to-weight ratio, 1×10^{-4}; engine specific impulse, 8000 seconds; Lagrangian multiplier λ_4, 0.

Specification of longer travel times merely results in the optimum transfer with an additional coast phase either in Earth's orbit before proceeding with the transfer or in Mars' orbit after completing the transfer. If much longer travel times (corresponding to transfers making more than 1 revolution about the sun) are specified, transfers with more than one sequence of propulsion, coast, propulsion could presumably be obtained. Transfers with such long travel times were not investigated in the present analysis.

The variation of the thrust angle along the trajectories presented in figure 1(a) is shown in figure 1(b). The thrust angle for the $C = 0$ transfer (290 days) is nearly tangential (again analogous to the Hohmann transfer for impulsive thrust). As travel time is decreased, increasingly larger radial components of thrust are introduced. The radial components are outward from the local horizontal for the near Earth phase of the trajectory and inward for the Mars phase. The thrust angle for the continuous-propulsion transfer is continuous, and the apparent discontinuity in figure 1(b) is only a result of presenting the thrust angle from $-\pi$ to π rather from 0 to 2π. In general, $d\psi/dt$ is positive during the propulsion phases of the flight.

The effect of travel time on the final- to initial-mass ratio m_f/m_0 is shown in figure 1(c) for the transfers with an optimum travel angle. As developed in the ANALYSIS, the highest mass ratio is obtained for the transfer with $C = 0$. Initially, travel time can be reduced from the optimum with only a

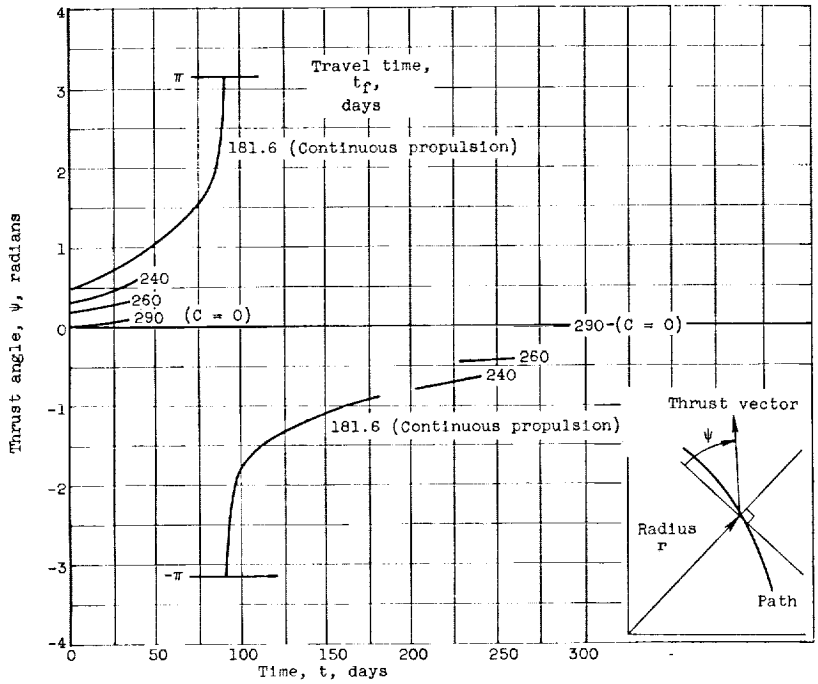

(b) Thrust angle.

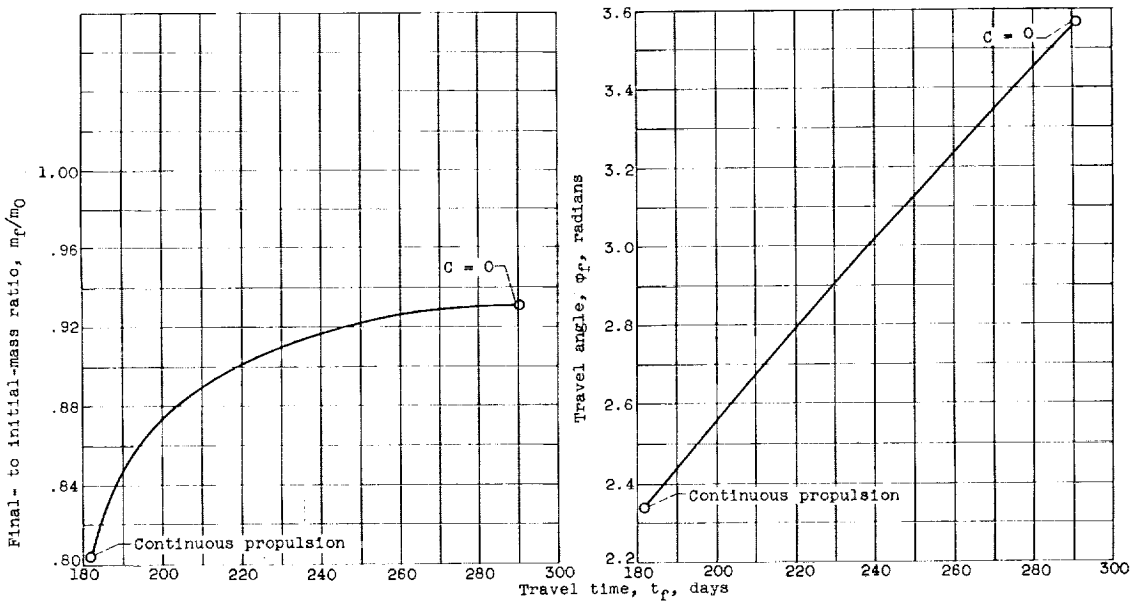

(c) Final mass ratio.

(d) Optimum travel angle.

Figure 1. - Concluded. Effect of travel time on Earth-Mars transfers. Initial thrust-to-weight ratio, 1×10^{-4}; engine specific impulse, 8000 seconds; Lagrangian multiplier λ_4, 0.

small decrease in mass ratio. However, as the travel time approaches that for the continuous-propulsion case, the mass ratio decreases rapidly.

The variation in the optimum travel angle with travel time is shown in figure 1(d). The planetary configuration required for an optimum-travel-angle transfer at a given travel time can be met once each synodic period.

Nonoptimum travel angles, $\lambda_4 \neq 0$. - The transfers presented in figure 1 all possess an optimum travel angle. At each travel time it is also possible to make transfers with travel angles both larger and smaller than the optimum, at the expense of increased propellant consumption. Thus, for one-way missions it will generally be desirable to use transfers with an optimum travel angle. For round-trip missions of specified duration, however, it will generally be desirable to use nonoptimum travel angles for both the outbound and inbound segments of the mission; this is discussed later.

The range of travel angles that can be achieved at a particular travel time for an Earth-Mars transfer is illustrated graphically in figure 2. The flights shown are those very near the maximum and minimum and the optimum travel angle for a travel time of 240 days. The limiting cases of maximum and minimum travel angle require continuous propulsion, and all the intervening travel angles are obtained with varying lengths of coast phase. The longest travel angle is achieved by initially moving inside Earth's orbit before moving out to Mars. The shortest travel angle is obtained by moving out beyond the orbit of Mars in the latter phase of the trajectory and entering from higher radii. This phenomenon cannot be noted clearly because of the limited scale of figure 2.

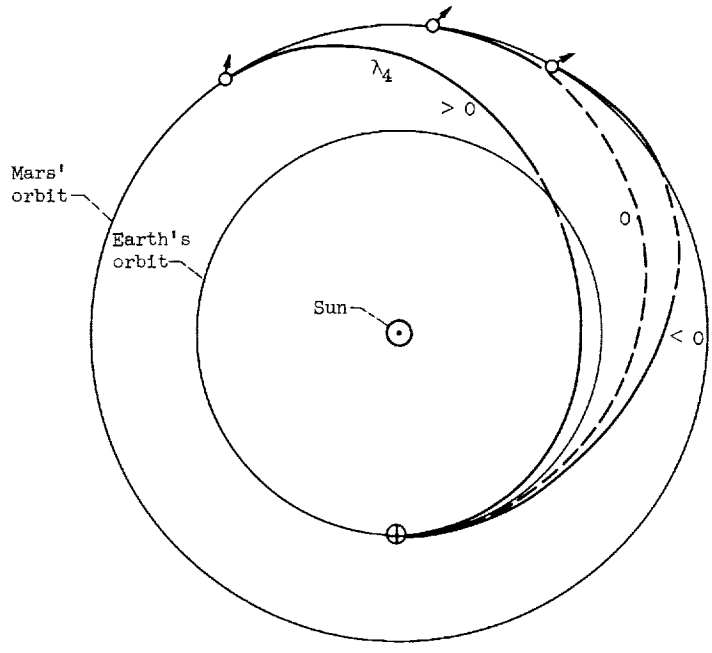

Figure 2. - Comparison of Earth-Mars transfers with optimum and nonoptimum travel angles. Travel time, 240 days; initial thrust-to-weight ratio, 1×10^{-4}; engine specific impulse, 8000 seconds.

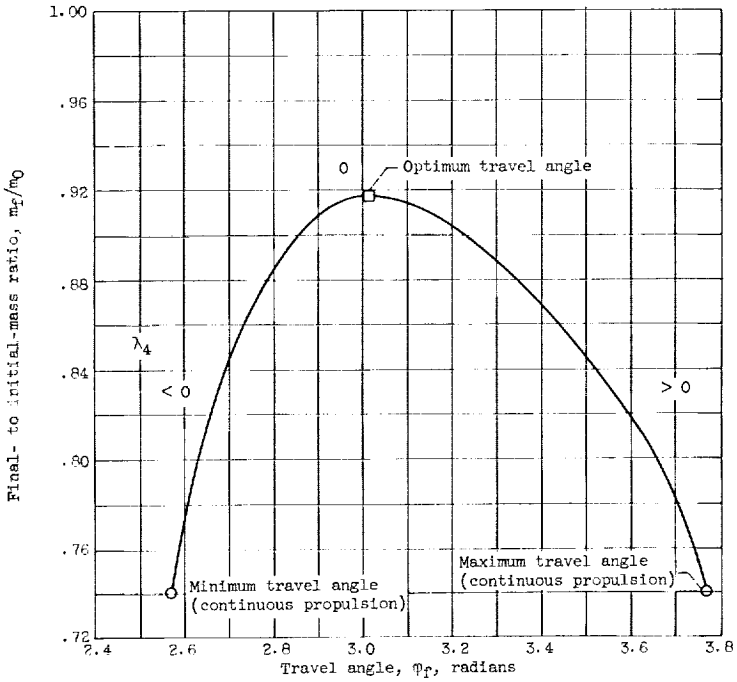

Figure 3. - Effect of travel angle on final- to initial-mass ratio for Earth-Mars transfers. Travel time, 240 days; initial thrust-to-weight ratio, 1×10^{-4}; engine specific impulse, 8000 seconds.

The effect of travel angle on m_f/m_0 is presented in figure 3 for the reference set of engine parameters and a travel time of 240 days. Figure 3 demonstrates the optimizing nature of $\lambda_4 = 0$ trajectories. Travel angles larger than the optimum value are obtained with positive values of λ_4, and travel angles shorter than the optimum are obtained with negative values of λ_4.

Performance map for reference engine parameters. - From data similar to those presented in figure 3 for a range in travel time, a map of possible Earth-Mars trajectories can be obtained. Such a performance map is presented in figure 4 for the reference engine parameters. For convenience, travel angle is presented as a function of travel time with the final- to initial-mass ratio as a parameter. The continuous-propulsion flights form the outer boundary of the map. Flights inside the boundary have a coast phase, while those outside the boundary are not achievable with the reference engine parameters. Also, in the upper right portion of the map the flights have an initial as well as an intermediate coast phase. Similarly, in the lower right portion of the map flights occur with a final as well as an intermediate coast phase. The double-coast-phase trajectories are not new trajectories, but are trajectories obtained at shorter travel times and angles extended with an initial or final coast phase. The boundaries of these multiple coast regions have not been evaluated because they are characterized by $k = 0$ either at the start or end of the transfer, which is a very sensitive two-point boundary value problem that cannot be solved accurately without special machine program modifications.

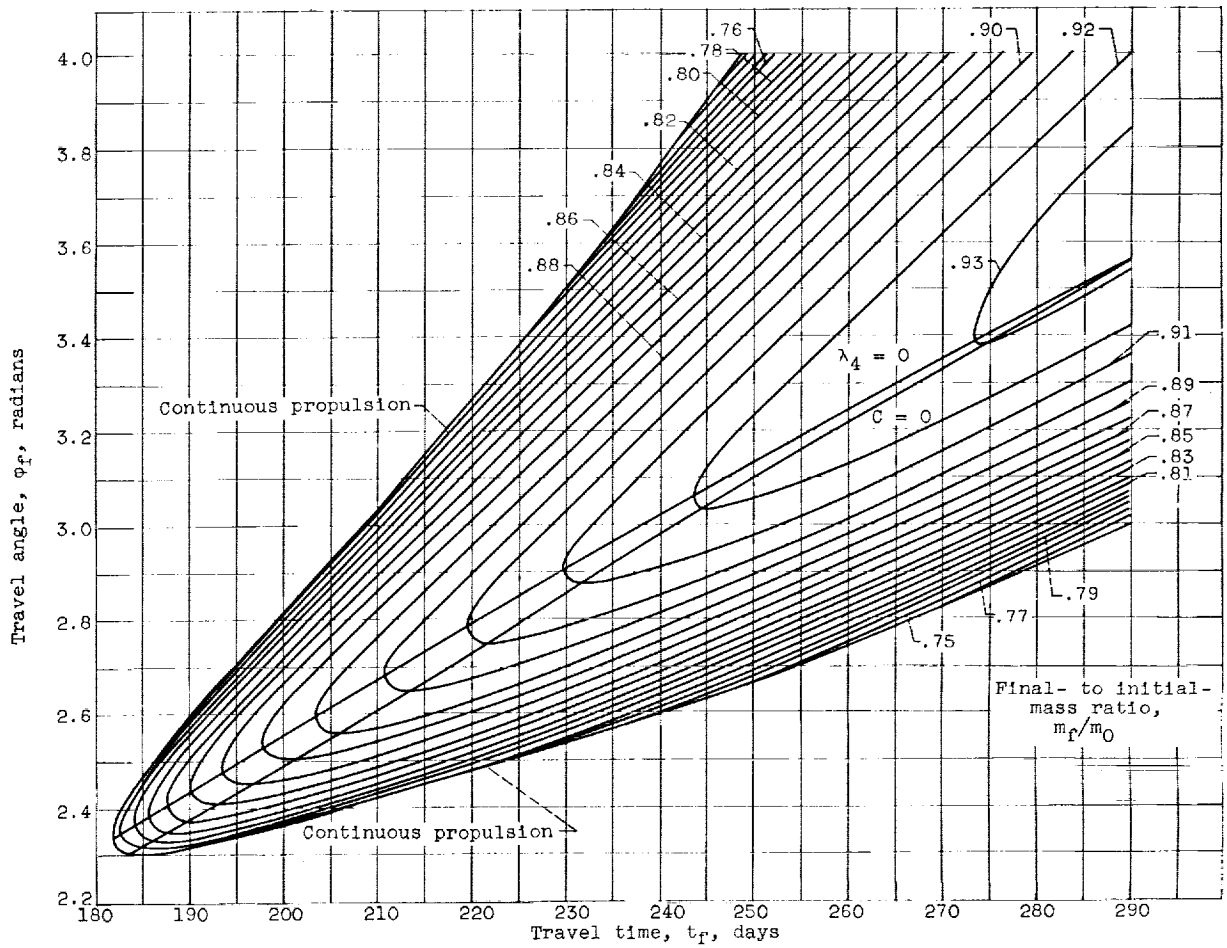

Figure 4. - Effect of travel time on travel angle for various values of final- to initial-mass ratio for Earth-Mars transfers. Initial thrust-to-weight ratio, 1×10^{-4}; engine specific impulse, 8000 seconds.

Curves indicating the $C = 0$ and $\lambda_4 = 0$ trajectories are superimposed on the map; once again the optimum nature of these trajectories (as given by the transversality condition in the ANALYSIS) is apparent. The $\lambda_4 = 0$ curve connects the vertical tangents to the mass-ratio curves; this produces the optimum travel angle for each travel time. Similarly, the $C = 0$ curve connecting the horizontal tangents gives the optimum travel time for each travel angle. The highest mass ratio, 0.931, is obtained at the intersection of the $\lambda_4 = 0$ and and the $C = 0$ curves. This is the 290-day transfer described in detail in figure 1; as mentioned previously, longer travel times were not investigated in the present analysis.

Engine parameters. - The data presented thus far have all been for the reference set of engine parameters. The effect of thrust-to-weight ratio on Earth-Mars transfers with optimum travel angles is shown in figure 5 for a specific impulse of 8000 seconds. For each thrust-to-weight ratio, travel time is varied from the minimum time (continuous-propulsion flights) to the time

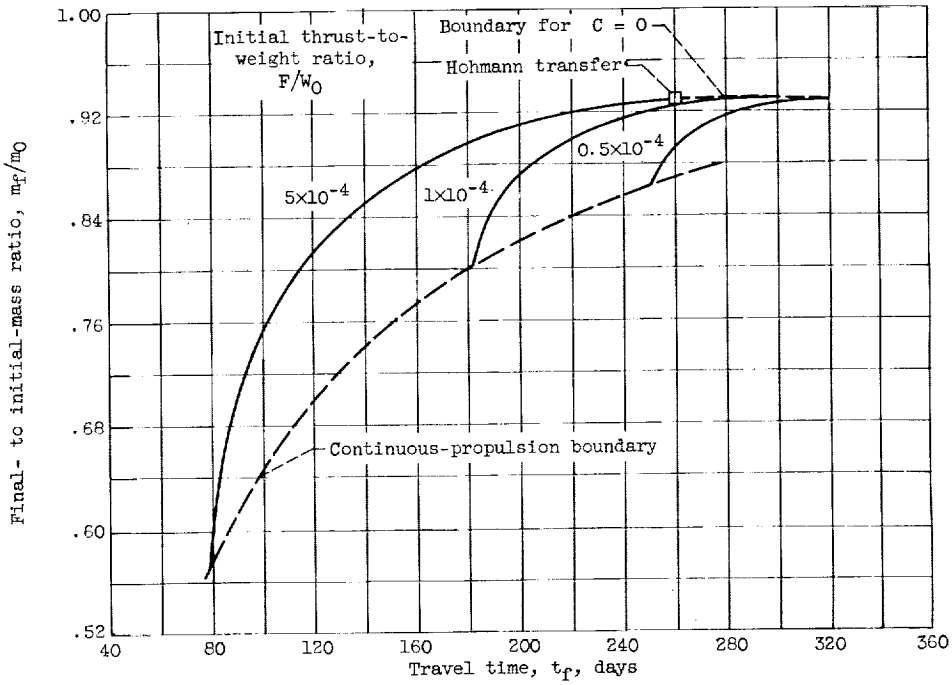

Figure 5. - Effect of travel time and thrust-to-weight ratio on final- to initial-mass ratio for Earth-Mars transfers. Engine specific impulse, 8000 seconds; Lagrangian multiplier λ_4, 0.

maximizing the final- to initial-mass ratio (flights with C = 0). The predominant effect of thrust-to-weight ratio is the widening of the band of achievable travel times as thrust-to-weight ratio is increased. In particular, achieving short travel times requires relatively high thrust-to-weight ratios. Also, at the long travel times, the optimum transfers (C = 0) approach the Hohmann transfer as thrust-to-weight ratio is increased.

The effect of specific impulse on Earth-Mars transfer trajectories is shown in figure 6(a) for a thrust-to-weight ratio of 0.5×10^{-4}. Again, the trajectories have optimum travel angles, and the travel time is varied from the continuous-propulsion case to that for a maximum mass ratio. The specific impulse, of course, has a major effect on the required mass ratio, but a change in specific impulse has only a minor effect on the trajectory used. For example, a change in specific impulse has almost no effect on the travel angle required for a transfer of given duration, as indicated by the nearly vertical constant travel-angle curves in figure 6(a). A secondary effect of specific impulse is to widen the range of travel times available as the specific impulse is reduced. This is due to the greater mass expenditure and hence increased average acceleration at the lower specific impulses and is thus similar to the effect of thrust-to-weight ratio shown in figure 5.

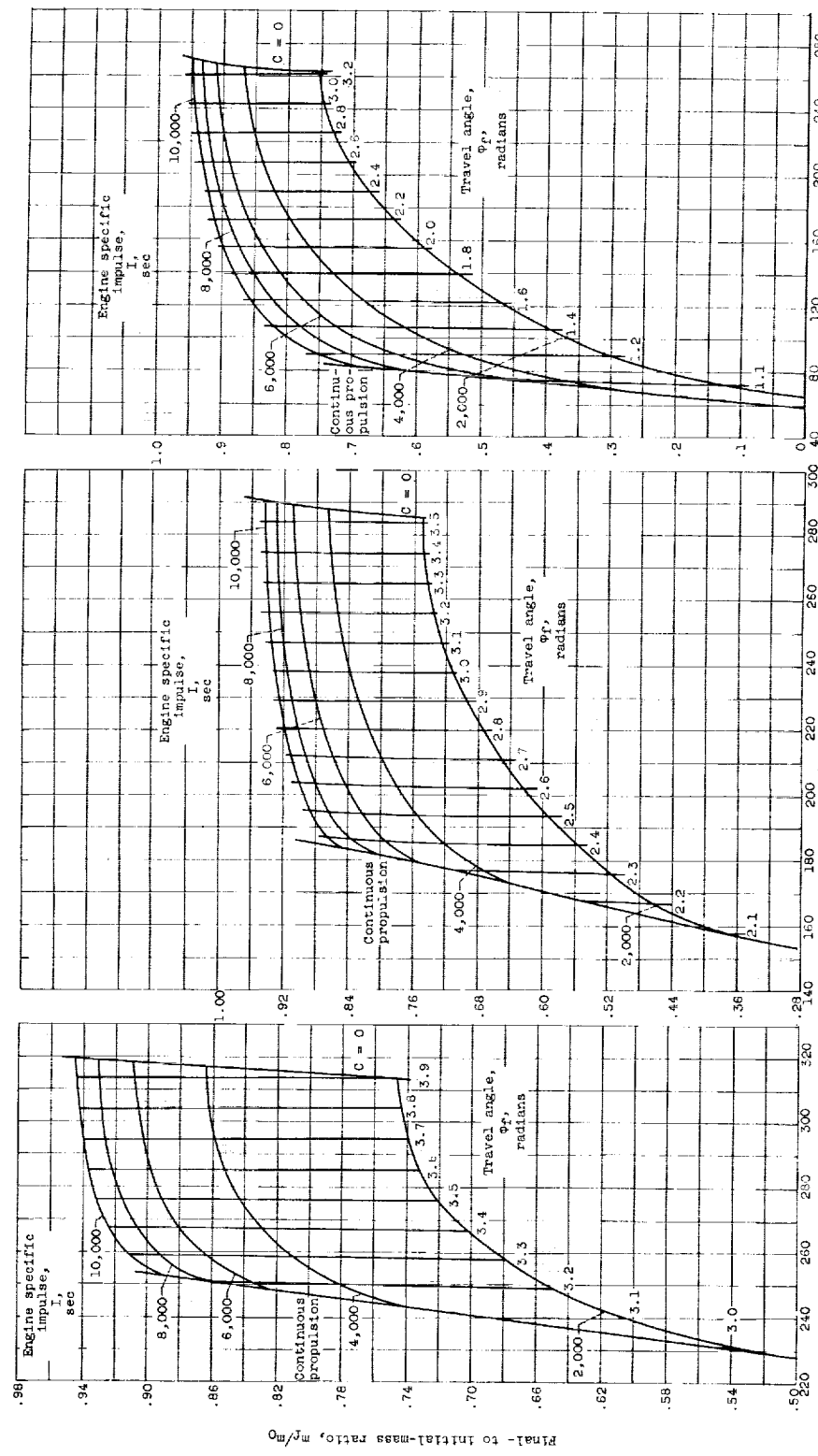

Figure 6. - Effect of travel time and specific impulse on final- to initial-mass ratio for Earth-Mars transfers. Lagrangian multiplier λ_4, 0.

Trajectory Charts for One-Way Missions

Figures 6 and 7 summarize the trajectory data that have been obtained for Earth-Mars transfers. All the data are for transfers with an optimum travel angle, and the travel time varies from the minimum time for the continuous-propulsion case to the time for the maximum final- to initial-mass ratio. In figure 6, the final- to initial-mass ratio is presented as a function of travel time and specific impulse for thrust-to-weight ratios of 0.5×10^{-4}, 1×10^{-4}, and 5×10^{-4}. In figure 7, the apportionment of travel time into initial propulsion time, coast time, and final propulsion time is presented for the same range of engine parameters. Figures 8 and 9 present similar data for Mars-Earth trajectories with optimum transfer angles. Comparison of figures 6 and 7 with figures 8 and 9 indicates the similarity between Earth-Mars and Mars-Earth trajectories.

Comparison with Variable-Thrust Trajectories

In order to compare the results of this analysis with the results for the variable-thrust engine of reference 2, two modifications must be made. The first concerns finding the optimum I for a given jet power and travel time. The optimum I can be obtained as part of the variational solution as shown in reference 5 or by simply constructing the constant jet power-to-initial mass ratio P/M_0 envelope of curves at constant F/W_0 and I. The latter method has been used here and is illustrated in figure 10. The second modification concerns the boundary conditions. For the comparison, Mars' orbit was assumed to be an ellipse, of known eccentricity and semilatus rectum, coplanar to Earth's circular orbit. Transfers to the Martian ellipse were made with an optimum travel angle to the best point on the ellipse for the given travel time. The transversality conditions for these end conditions are developed and discussed in detail in appendix C.

For comparison, a nominal value of 0.04808 kilowatt per kilogram for P/M_0 (which corresponds to $(F/W_0)I = 1$) was assumed, and F/W_0 and I were varied to construct the envelope curve. The resulting propellant fractions are shown in figure 10, where they are also compared with the variable-thrust engine results. There is very little difference between the two curves at high values of t_f, but the inherent advantage of the variable-thrust engine becomes more apparent as the travel time is reduced. This difference, at short times, becomes about 5 percent of the initial mass. The significance of these differences cannot fully be assessed until more is known about these engines. The propellant requirements of both engine types, however, are valuable as a guide in design and evaluation.

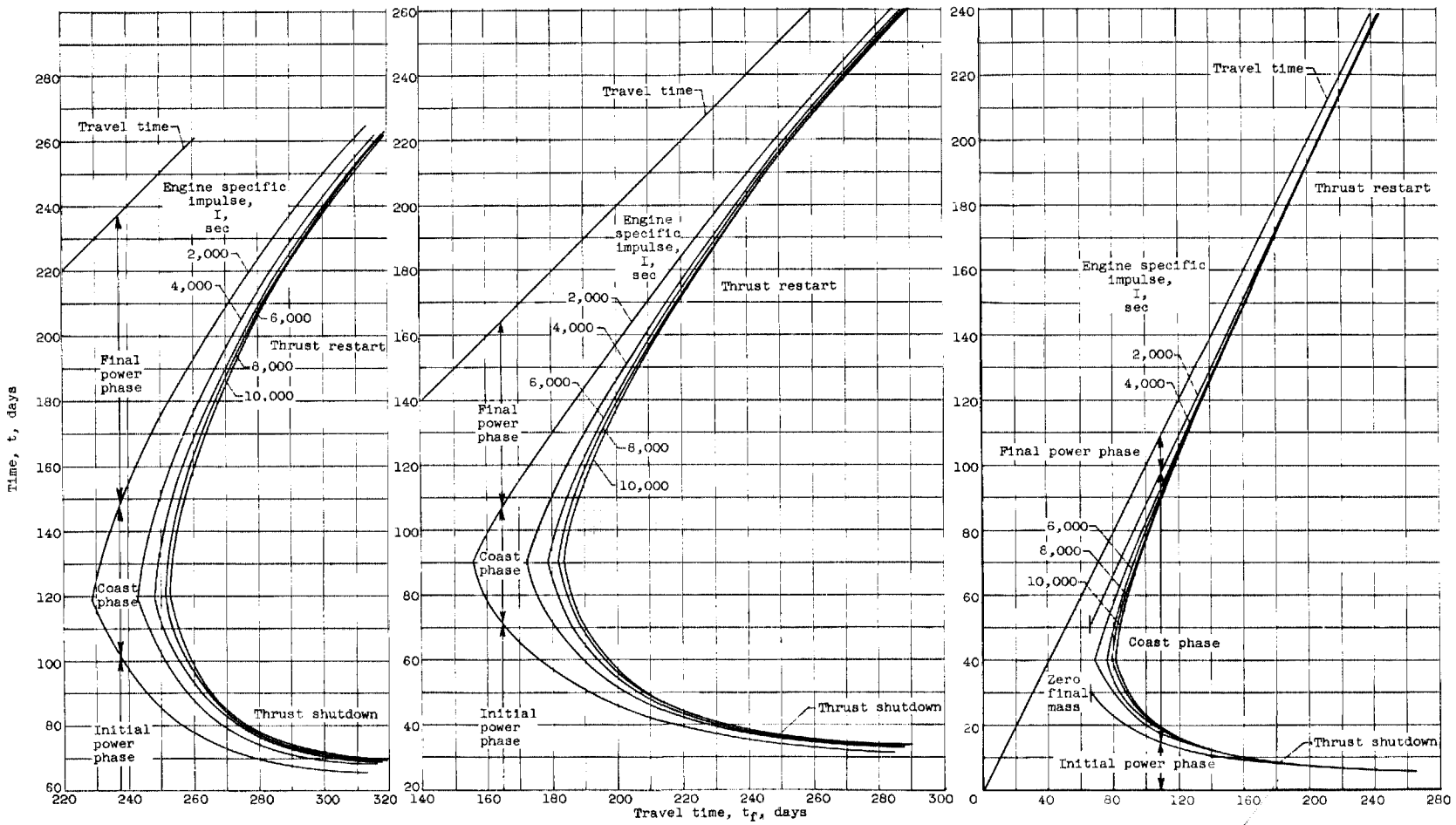

(a) Initial thrust-to-weight ratio, 0.5×10^{-4}.

(b) Initial thrust-to-weight ratio, 1×10^{-4}.

(c) Initial thrust-to-weight ratio, 5×10^{-4}.

Figure 7. - Apportionment of travel time for Earth-Mars transfers. Lagrangian multiplier λ_4, 0.

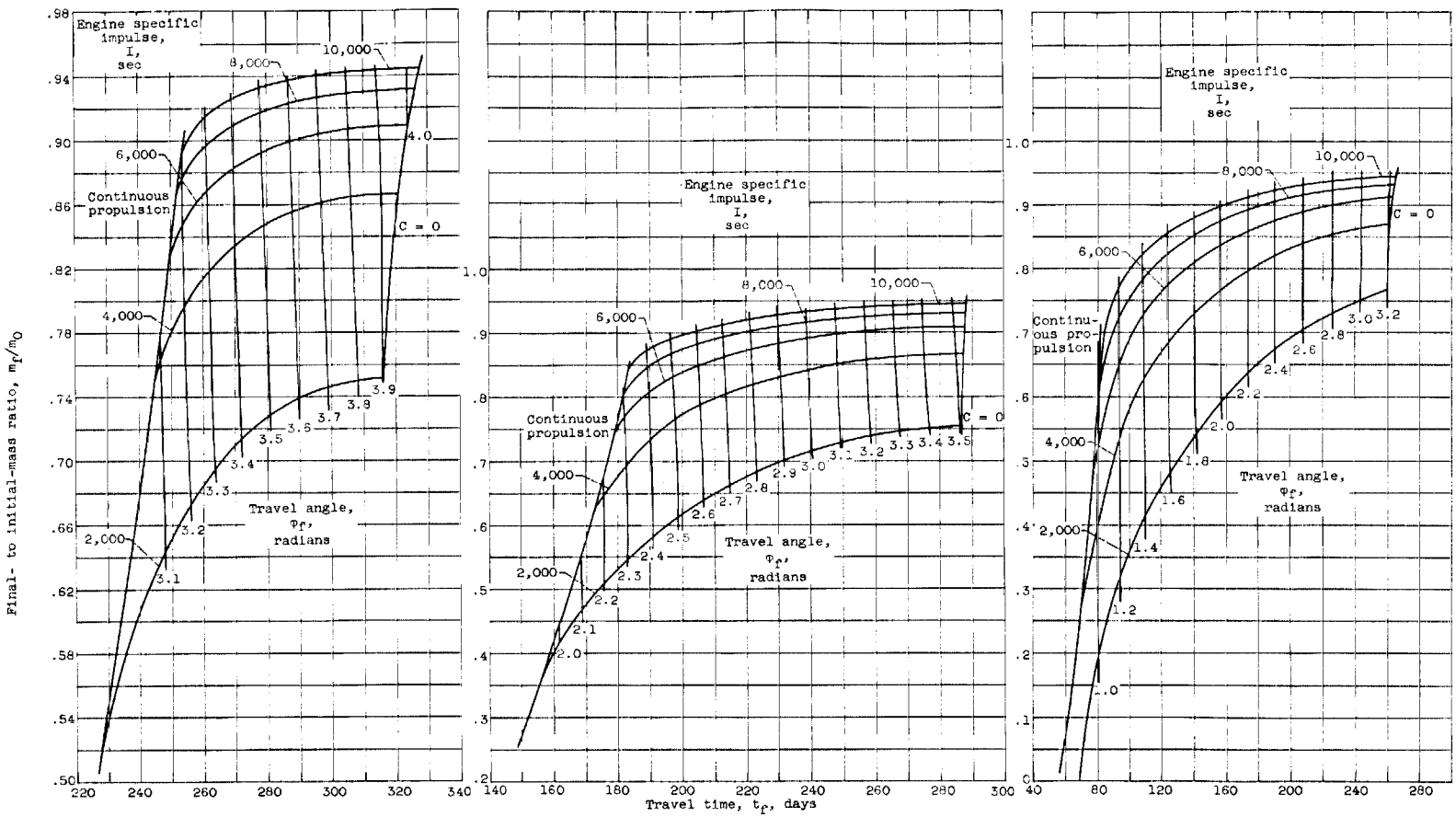

(a) Initial thrust-to-weight ratio, 0.5×10^{-4}.

(b) Initial thrust-to-weight ratio, 1×10^{-4}.

(c) Initial thrust-to-weight ratio, 5×10^{-4}.

Figure 8. - Effect of travel time and specific impulse on final- to initial-mass ratio for Mars-Earth transfers. Lagrangian multiplier λ_4, 0.

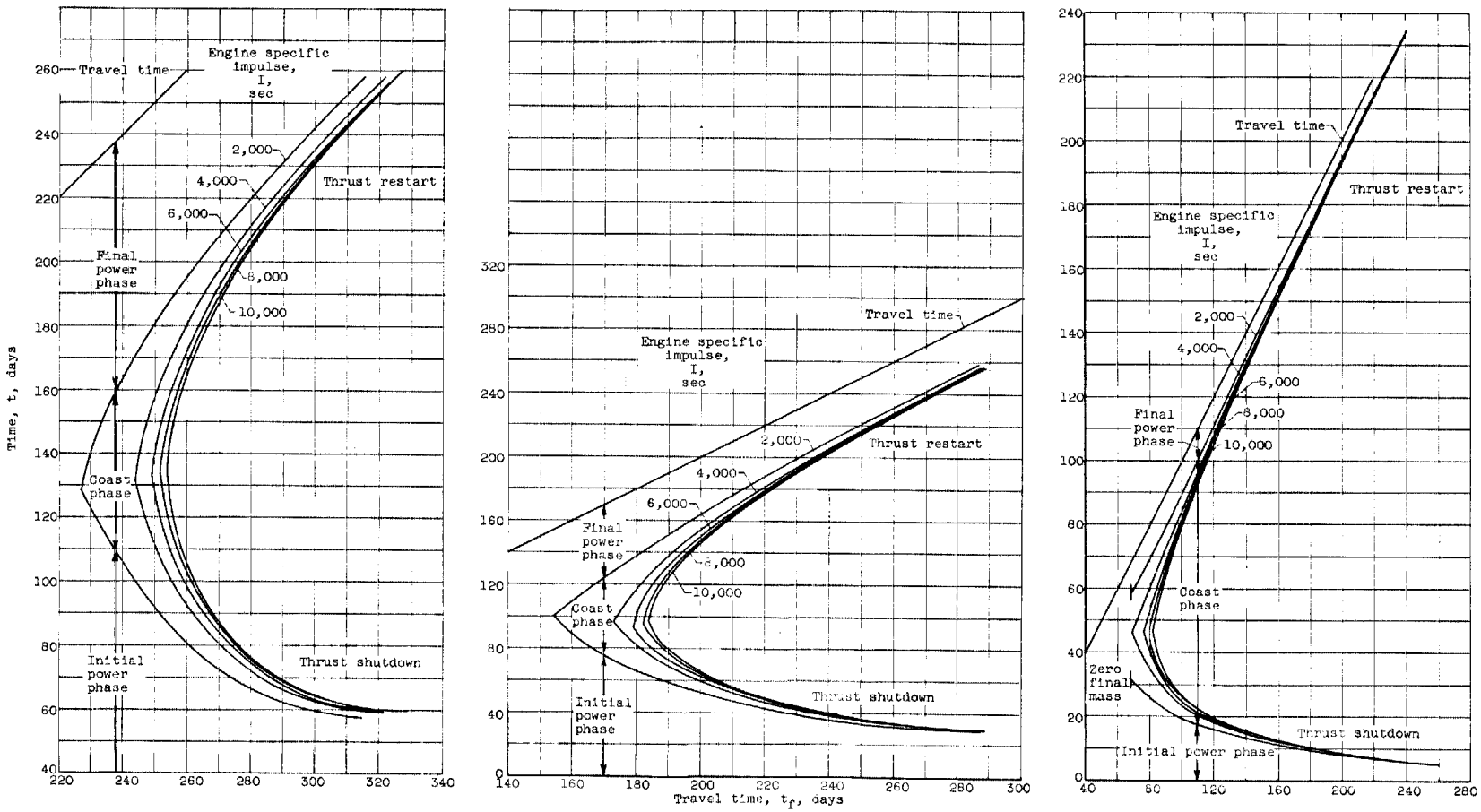

(a) Initial thrust-to-weight ratio, 0.5×10^{-4}.

(b) Initial thrust-to-weight ratio, 1×10^{-4}.

(c) Initial thrust-to-weight ratio, 5×10^{-4}.

Figure 9. - Apportionment of travel time for Mars-Earth transfers. Lagrangian multiplier λ_4, 0.

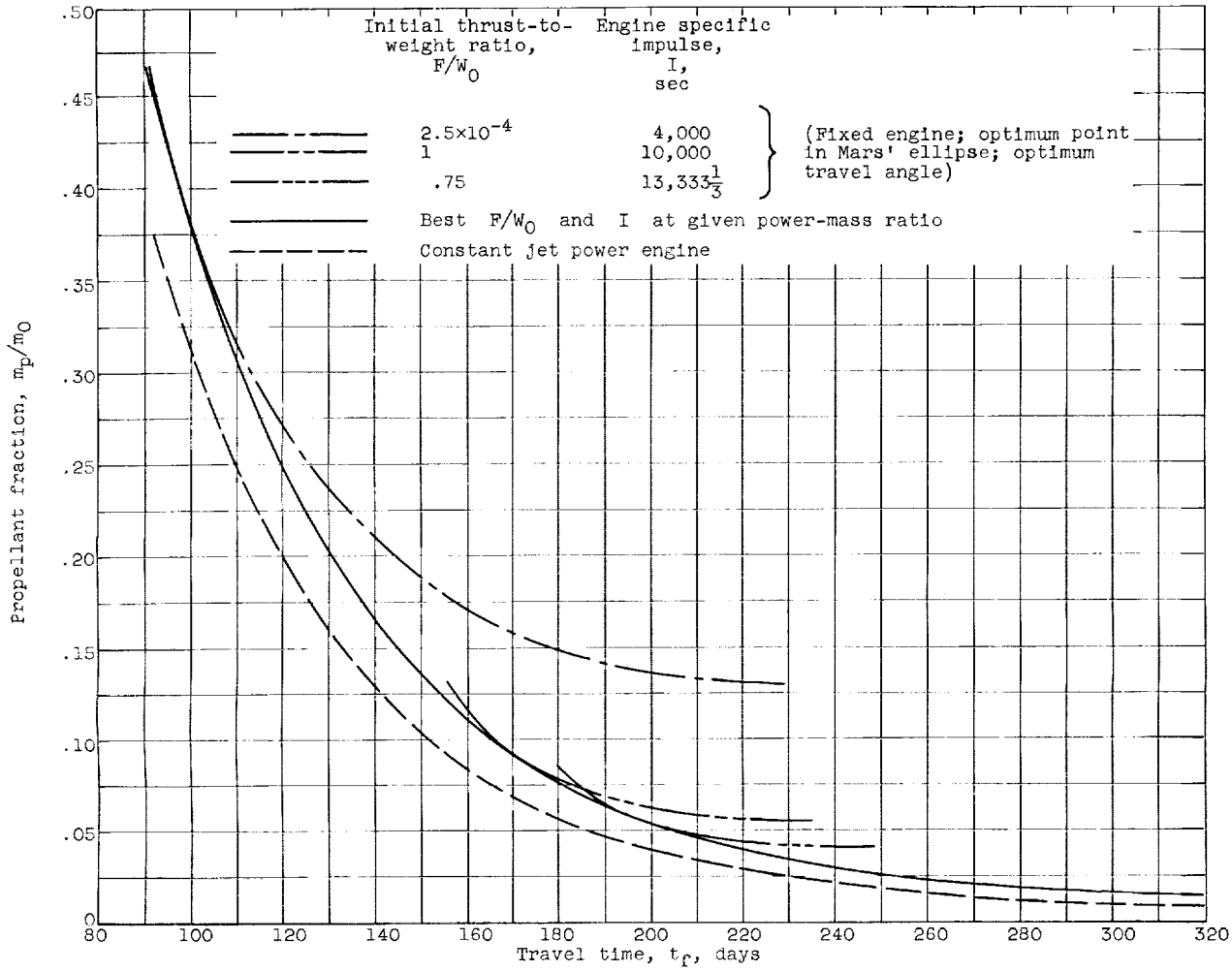

Figure 10. - Comparison of fixed-design engine and constant jet power engine for Earth-Mars transfers. Jet power-to-initial mass ratio, 0.04808 kilowatt per kilogram; $(F/W_0)I = 1$.

Round-Trip Calculations

As pointed out previously, this report does not contain sufficient data for a comprehensive study of round-trip, Earth-Mars missions. A limited amount of nonoptimum-travel-angle data has been computed, however, and will be used to help illustrate a method for computing round trips that uses performance charts of the type shown in figure 4. In the calculation of round trips of given duration and waiting time, the travel time and travel angle for the outbound transfer may be selected at will. Once this has been done, however, the same variables for the inbound transfer must satisfy the rendezvous equations

$$\left.\begin{aligned} t_m - t_w &= t_{out} + t_{in} \\ t_m\omega_E - t_w\omega_M &= \varphi_{out} + \varphi_{in} \end{aligned}\right\} \tag{35}$$

where

t_m round-trip mission time

t_w waiting time

t_{out} outbound travel time

t_{in} inbound travel time

ω_E Earth's angular velocity

ω_M Mars' angular velocity

φ_{out} outbound travel angle

φ_{in} inbound travel angle

In view of the rendezvous equations it can be seen that optimum-travel-angle transfers can be used only for special combinations of t_w and t_m. To optimize the round trip, for specified t_m and t_w the pair of outbound parameters (t_{out}, φ_{out}) must be found that maximizes the mass at return to Earth. Such a problem is, in principle, within the scope of the indirect method of the calculus of variations. As such, however, it is beyond the scope of this report.

To solve this same problem by use of performance maps such as the one presented in figure 4, a selection is first made of F/W_0, I, t_{out}, and φ_{out}. From an appropriate performance map, the corresponding value of $(m_f/m_0)_{out}$ can be read. Thus the thrust-to-weight ratio at Mars arrival, $(F/W_0)(m_0/m_f)$, will be known and can be used with data (such as those found in ref. 8) to find the mass ratio required to spiral into and out of an orbit about Mars. Thus, the value of $(F/W_0)_{in}$ can be computed and can be used together with t_{in} and φ_{in} as determined from equations (35) to obtain the necessary value of $(m_f/m_0)_{in}$ from an appropriate inbound performance map.

In order to minimize the number of performance charts required, the first choice of $(t,\varphi)_{out}$ can be made such that $(F/W_0)_{in}$ has a value corresponding to that for one of the inbound performance maps that is available. Furthermore, it should be noted from figure 4 that a variety of values for $(t,\varphi)_{out}$ can be selected at the same value of $(m_f/m_0)_{out}$. Since all such cases will use the same inbound performance chart, it is possible to find the optimum value of $(t,\varphi)_{out}$ for a given value of $(m_f/m_0)_{out}$ by use of only two performance maps. This latter procedure is illustrated in figure 11, where all the values of $(t,\varphi)_{in}$

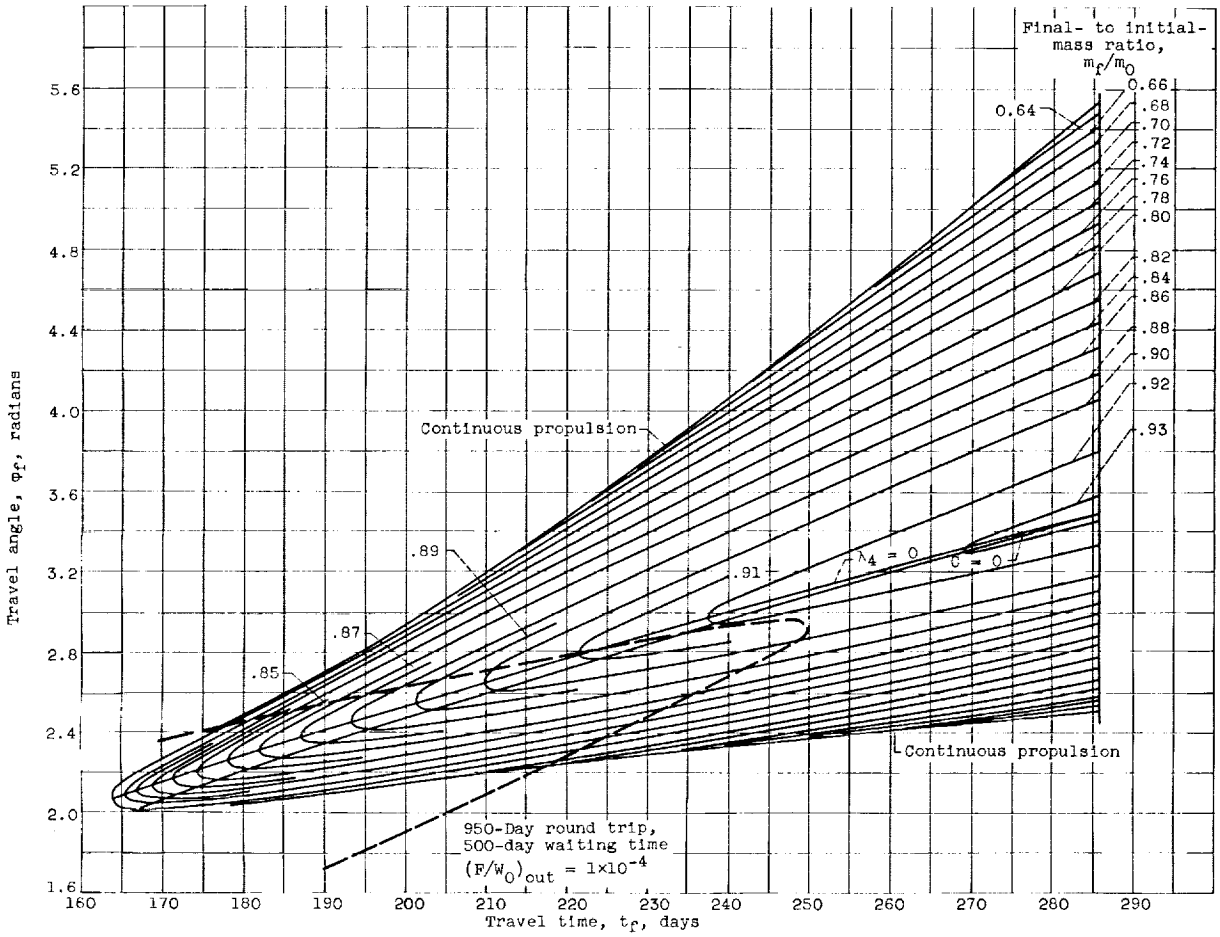

Figure 11. - Effect of travel time on travel angle for various values of final- to initial-mass ratio for Mars-Earth transfers. Initial thrust-to-weight ratio, 1.25×10^{-4}; engine specific impulse, 8000 seconds.

along the dashed curve were computed from equations (35) by use of $t_m = 950$, $t_w = 500$, and a series of outbound trips taken from figure 4 at $(m_f/m_0)_{out} = 0.875$. The value of $(m_f/m_0)_{out} = 0.875$ has been selected so that, with $(F/W_0)_{out} = 1\times10^{-4}$, $(F/W_0)_{in} = 1.25\times10^{-4}$, and $I = 8000$ seconds (figs. 4 and 11), sufficient propellant was available to spiral into and out of an orbit about Mars at $1.1 \times r_M$. From figure 11 it can be seen that the best trip of this type occurs when the dashed curve becomes tangent to one of the mass-ratio curves for the inbound trip. The details of the best case from figure 11 are given in the following table:

	Time, t, days	Polar angle, φ, radians	Final- to initial-mass ratio, m_f/m_0
Outbound	209	2.550	0.875
Spiral in	36.9	.337	.954
Park	430.5	3.938	1
Spiral out	32.6	.298	.958
Inbound	241	2.935	.919
Overall	950	10.058	.735

The case shown in the aforementioned table is the best possible for the chosen values of F/W_0, I, t_m, t_w, and $(m_f/m_0)_{out}$. In order to find the optimum value of $(m_f/m_0)_{out}$, the basic procedure illustrated by figure 11 . 1 have to be repeated for other values of $(m_f/m_0)_{out}$, and each new value would require a different inbound performance map.

One advantage of the method presented here is that it allows the computation of optimum round trips for many different combinations of t_w and t_m without any change in the number of performance maps required. Should it be necessary to investigate many different values of $(F/W_0)_{out}$ and I, however, the number of charts required could become prohibitive.

CONCLUDING REMARKS

The calculus of variations has been used to derive differential equations that define planar, two-body, optimum trajectories for given boundary conditions. In the derivation, it is assumed that the gravitational field is of the inverse-square type and that the engine operates with fixed thrust and specific impulse but may be shut down and restarted at will. The resulting equations have been programed for an IBM 704 computer along with a three-variable Newton-Raphson iteration scheme to overcome the inherent two-point boundary value problem. This machine program has been successfully applied in an investigation of both Earth-Mars and Mars-Earth transfer trajectories with a range of values for initial thrust-to-weight ratio and engine specific impulse.

In order to compare results with those for continuously variable thrust as presented in reference 2, a special series of calculations has been made for transfers to an elliptical Martian orbit from a circular Earth orbit. The final comparison of these results shows that the two solutions differ very little at long travel times and that the variable-thrust solution has an advantage at short travel times that amounts to about 5 percent of the initial mass for the case chosen.

Most of the data presented have the optimum travel angle at each travel time and are, therefore, most applicable to the study of one-way transfers. Sufficient nonoptimum-travel-angle data have been presented to illustrate a possible method for computing round-trip trajectories.

Lewis Research Center
National Aeronautics and Space Administration
Cleveland, Ohio, September 4, 1962

APPENDIX A

SYMBOLS

C	first integral to Euler-Lagrange equations
E	Weierstrass excess function
e	eccentricity
F	$\sum_{i=1}^{6} f_i \lambda_i$
F/W_0	initial thrust-to-weight ratio
f	constraint equation
g	function of initial and final conditions to be minimized
I	engine specific impulse, sec
J	functional to be minimized by variational methods
K	constant of integration
$\mathcal{K}, \mathcal{L}, \mathcal{M}$	transversality functions for elliptic orbits
k	function defining coast phases
L	function associated with analytical solution for coast phases
m	mass, kg
P/M_0	jet power-to-initial mass ratio, kw/kg
p	semilatus rectum, m
r	radius, m
t	time, days
t_f	travel time, days
t_m	mission time, days
t_w	wait time, days
u	radial velocity, m/sec
V_j	engine exhaust velocity, 9.80665 I, m/sec

Z	dummy variable
α	argument of pericenter, radians
β	propellant flow rate, kg/sec
θ	true anomaly, radians
λ	Lagrangian multiplier
μ	gravitational constant, m^3/sec^2
φ	polar angle, radians
φ_f	travel angle, radians
ψ	thrust angle measured from normal to radius, radians
ω	polar angular velocity, radians/sec

Subscripts:

des	design
E	Earth
f	final ($t = t_f$)
M	Mars
m	mission
p	propellant
w	waiting
0	$t = 0$

Superscripts:

.	d/dt
'	$d/d\varphi$

APPENDIX B

SOLUTION OF EULER-LAGRANGE EQUATIONS DURING COAST

The purpose of this appendix is to derive analytical solutions for the following system of equations:

$$\dot{\lambda}_1 - 2\dot{\varphi}\lambda_2 + \lambda_3 = 0 \tag{B1}$$

$$\dot{\lambda}_2 - \frac{\dot{r}}{r}\lambda_2 + 2\dot{\varphi}\lambda_1 + \frac{\lambda_4}{r} = 0 \tag{B2}$$

$$\lambda_3 = -\frac{1}{\dot{r}}(\ddot{r}\lambda_1 + r\ddot{\varphi}\lambda_2 + \dot{\varphi}\lambda_4 + C) \tag{B3}$$

$$\ddot{r} = r(\dot{\varphi})^2 - \frac{\mu}{r^2} \tag{B4}$$

$$r\ddot{\varphi} = -2\dot{r}(\dot{\varphi}) \tag{B5}$$

which apply during the coast phase. Equations (B4) and (B5) have the well-known solutions:

$$r = \frac{p}{1 + e\cos(\varphi - \alpha)} \tag{B6}$$

and

$$r^2\dot{\varphi} = \sqrt{\mu p} \tag{B7}$$

Changing the independent variable in equations (B1) and (B2) from t to φ leads to

$$\lambda_1'\dot{\varphi} - 2\dot{\varphi}\lambda_2 + \lambda_3 = 0 \tag{B8}$$

and

$$\lambda_2'\varphi - \frac{\dot{r}}{r}\lambda_2 + 2\dot{\varphi}\lambda_1 + \frac{\lambda_4}{r} = 0 \tag{B9}$$

where $\lambda_1' = d\lambda_1/d\varphi$, and so forth. Substitution of equation (B3) into (B8) results in:

$$\lambda_1'\dot{\varphi}\dot{r} - (2\dot{\varphi}\dot{r} + r\ddot{\varphi})\lambda_2 - \ddot{r}\lambda_1 - C - \dot{\varphi}\lambda_4 = 0$$

From equation (B5),

$$2\dot{\varphi}\dot{r} + r\ddot{\varphi} = 0$$

Therefore,

$$\lambda_1' - \frac{\ddot{r}}{\dot{r}\dot{\varphi}}\lambda_1 = \frac{C}{\dot{r}\dot{\varphi}} + \frac{\lambda_4}{\dot{r}} \tag{B10}$$

By use of relations (B6) and (B7), equation (B10) can be integrated to give

$$\lambda_1 = \frac{Cp^2}{\mu e} L \sin\theta - \frac{\lambda_4}{e}\sqrt{\frac{p}{\mu}}\cos\theta + K_1 \sin\theta \tag{B11}$$

where

$$L = \int_0^{\theta} \frac{d\theta}{\sin^2\theta(1 + e\cos\theta)^2}$$

$$= \frac{e}{1 - e^2}\left[\frac{\sin\theta}{(1 + e\cos\theta)^2} + \frac{(1 + 2e^2)\sin\theta}{(1 - e^2)(1 + e\cos\theta)} - \frac{6e\tan^{-1}\left(\frac{\sqrt{1 - e^2}\tan\frac{\theta}{2}}{1 + e}\right)}{\left(1 - e^2\right)^{3/2}}\right]$$

$$- \frac{\cot\theta}{(1 + e\cos\theta)^2} \qquad \text{for } 0 < e < 1$$

$\theta = \varphi - \alpha$ and K_1 is a constant of integration. In evaluating L, only the elliptical case has been presented because of its frequent occurrence. Substituting equation (B11) into equation (B9) and integrating lead to

$$\lambda_2 = \frac{1}{1 + e\cos\theta}\left\{\frac{Cp^2}{\mu e^2}\left[L(1 + e\cos\theta)^2 + \cot\theta\right] + \lambda_4\left(\frac{2}{e} + \cos\theta\right)\right.$$

$$\left. \times \sin\theta\sqrt{\frac{p}{\mu}} + \frac{K_1(1 + e\cos\theta)^2}{e} - K_2\right\} \tag{B12}$$

where K_2 is a constant of integration. Equations (B6), (B7), (B11), (B12), and (B3) can then be used to determine λ_3.

Once the initial values of λ_1, λ_2, θ, p, and e are known, the constants K_1 and K_2 can be evaluated with equations (B11) and (B12). The problem that still remains is to solve for the λ_i at the second $k = 0$ point, the termination of coast. Since the λ_i are given as functions of θ, the value of θ

at $k = 0$ must be determined. Because of the transcendental nature of the equations, some iterative solution must be used to calculate θ at the termination of coast. A method based on finite differences, which converges rapidly to θ at $k = 0$, has been successfully applied. The subsequent power phase is numerically integrated by the methods previously discussed.

APPENDIX C

ELLIPTIC ORBIT BOUNDARY CONDITIONS

Transfers to an elliptic orbit are in principle no different from transfers to a circular orbit; however, certain parameters may be more convenient to use than others. In this analysis, the eccentricity, semilatus rectum, and perigee angle are used to describe the shape, size, and orientation of the ellipse with respect to the initial circular orbit. The true anamoly is used to identify the position of the vehicle in the final orbit. It should be noted here that the orientation of the ellipse gives rise to another degree of freedom - a circle has no orientation. The transformation of variables can be made through the use of the following equations:

$$\left.\begin{aligned} u &= \sqrt{\frac{\mu}{p}}\, e \sin\theta \\ \omega &= \sqrt{\frac{\mu}{p^3}}\,(1 + e\cos\theta)^2 \\ r &= \frac{p}{1 + e\cos\theta} \\ \varphi &= \theta + \alpha \end{aligned}\right\} \qquad (C1)$$

Substitution of the total derivatives of equations (C1) into the transversality expression (eq. (26)) gives

$$\begin{aligned} dJ = -dm_f + \Bigg[& \lambda_5\, dm + \left(\frac{u}{e}\lambda_1 + \frac{2r^2\omega\cos\theta}{p}\lambda_2 - \frac{r^2\cos\theta}{p}\lambda_3\right)de \\ & + \left(\frac{r}{p}\lambda_3 - \frac{u}{2p}\lambda_1 - \frac{3r\omega}{2p}\lambda_2\right)dp \\ & + \left(\frac{u\lambda_1}{\tan\theta} - \frac{2r^2 e\omega\sin\theta}{p}\lambda_2 + \frac{r^2 e\sin\theta\lambda_3}{p} + \lambda_4\right)d\theta + \lambda_4\, d\alpha + C\, dt \Bigg]_{t_0}^{t_f} \end{aligned} \qquad (C2)$$

or, for the case of fixed initial conditions,

$$dJ = \Big[(\lambda_5 - 1)dm + \mathcal{K}\, de + \mathcal{L}\, dp + \mathcal{M}\, d\theta + \lambda_4\, d\alpha + C\, dt\Big]_{t_f} = 0 \qquad (C3)$$

where $\mathcal{K}$, $\mathcal{L}$, and $\mathcal{M}$ are coefficients of de, dp, and $d\theta$ as defined by equation (C2). As previously discussed, a transfer is optimum with respect to a

particular variable if its coefficient is zero at the boundary. Consider, for example, transfers used in the comparison with the variable-thrust engine of reference 2. Here, each transfer was made with e_f, p_f, and t_f fixed; as previously discussed, $\lambda_{5,f} = 1$ was satisfied by scaling. In addition, $\mathscr{M} = 0$ and $\lambda_4 = 0$ were also satisfied. These transfers then have the optimum orientation α of the Martian ellipse (e,p), and the vehicle arrives at the optimum point on the final ellipse θ_f in the given time t_f. Because of the relation among orientation, true anomaly, and travel angle, the optimum orientation also implies optimum travel angle for some given θ_f. The two-point boundary value problem for this case is, therefore,

$$\left.\begin{array}{ll} \text{At } t = t_0 & \text{At } t = t_f \\ \lambda_1 & e = e_M = 0.093369 \\ \lambda_2 & p = p_M = 2.2581 \times 10^{11} \\ C & \mathscr{M} = 0 \end{array}\right\} \qquad \text{(C4)}$$

Another type of transfer that can be made is the same as that just described except that the point of arrival is nonoptimum θ. The optimum point of arrival $\mathscr{M} = 0$ is included in this class of transfers. This class of transfers also points out that there are two points on the final ellipse that have $\mathscr{M} = 0$ - maximum m_f and minimum m_f. Therefore, an additional test should be made to distinguish the two cases. Also, some points on the Martian ellipse are not achievable with all sets of engine parameters and are defined by the continuous-propulsion limits of the engine. In this case, the minimum m_f occurs at the continuous-propulsion points but is not defined by $\mathscr{M} = 0$. These characteristics of the elliptic orbit boundary are shown in figure 12, where both $\mathscr{M}$ and m_f/m_0 are given as functions of θ_f for an Earth-Mars transfer with $F/W_0 = 1 \times 10^{-4}$, $I = 10{,}000$ seconds and $t_f = 200$ days.

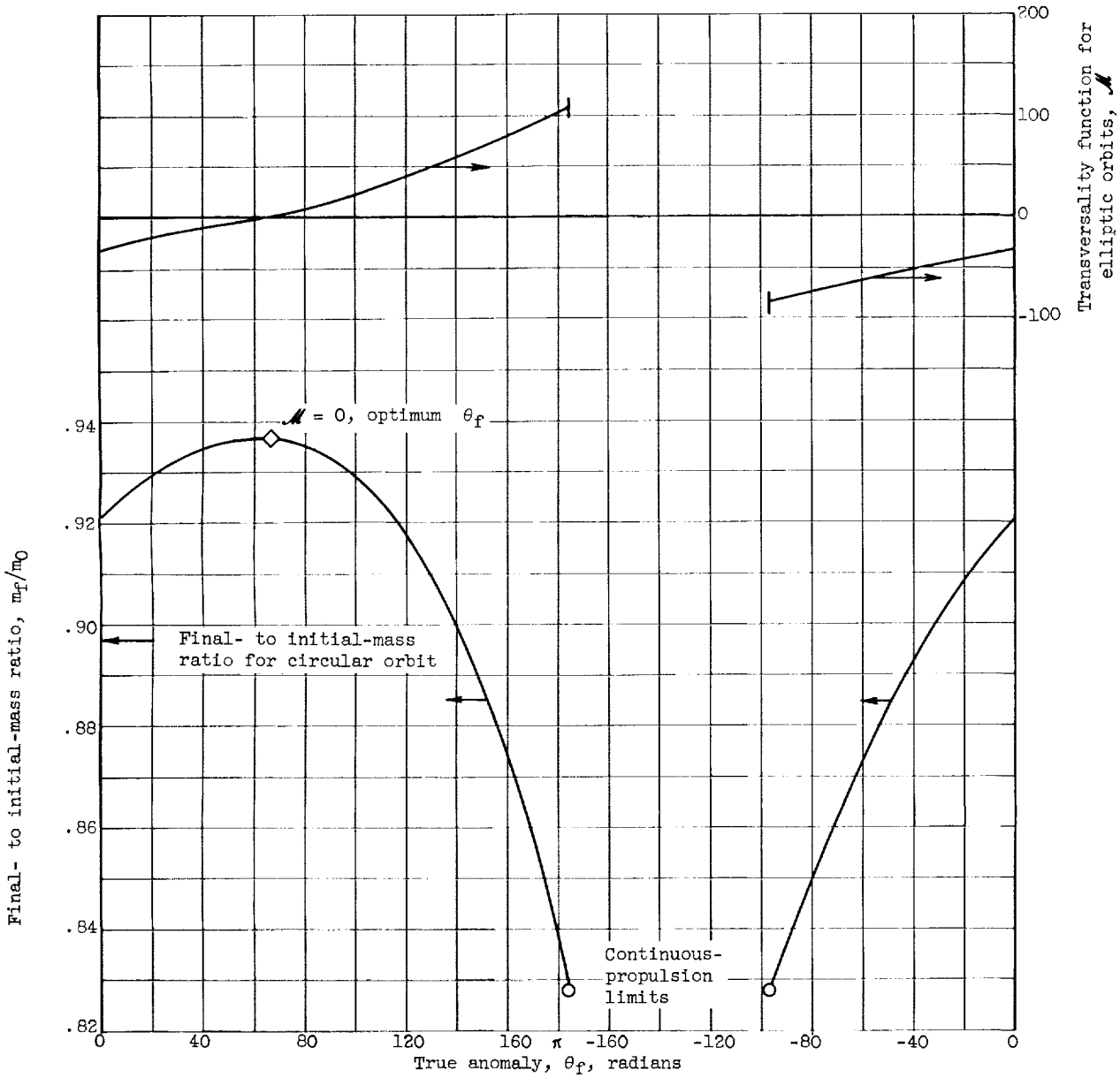

Figure 12. - Effect of true anomaly of elliptic Mars' orbit on final- to initial-mass ratio for Earth-Mars transfers. Travel time, 200 days; initial thrust-to-weight ratio, 1×10^{-4}; engine specific impulse, 10,000 seconds; Lagrangian multiplier λ_4, 0.

APPENDIX D

EQUATIONS FOR MINIMIZING TRAJECTORY

The following equations are required for the determination of the minimizing trajectory:

Equations of motion:

$$\dot{u} = -\frac{\mu}{r^2} + \omega^2 r + \frac{V_j \beta}{m} \sin \psi \tag{1a}$$

$$\dot{\omega} = -\frac{2u\omega}{r} + \frac{V_j \beta}{m} \frac{\cos \psi}{r} \tag{1b}$$

$$\dot{r} = u \tag{1c}$$

$$\dot{\varphi} = \omega \tag{1d}$$

where

$$m = -\beta \tag{1e}$$

Euler-Lagrange equations:

$$\dot{\lambda}_1 = 2\omega\lambda_2 - \lambda_3 \tag{7a}$$

$$\dot{\lambda}_2 = -2\omega\lambda_1 + \frac{u}{r}\lambda_2 - \frac{\lambda_4}{r} \tag{7b}$$

$$\dot{\lambda}_3 = -\left(\frac{2\mu}{r^3} + \omega^2\right)\lambda_1 + \dot{\omega}\lambda_2 \tag{7c}$$

where

$$\lambda_4 = \text{const}$$

$\sin \psi$ and $\cos \psi$ are given by

$$\sin \psi = \frac{\lambda_1}{+\sqrt{\lambda_1^2 + \lambda_2^2}} \qquad \cos \psi = \frac{\lambda_2}{+\sqrt{\lambda_1^2 + \lambda_2^2}} \tag{9}$$

β is given by

$$\left.\begin{aligned} \beta &= \beta_{des} \quad \text{for} \quad k \geq 0 \\ \beta &= 0 \quad \text{for} \quad k \leq 0 \end{aligned}\right\} \tag{24}$$

where

$$k = \frac{V_j}{m}(\lambda_1 \sin\psi + \lambda_2 \cos\psi) - \lambda_5 \tag{17a}$$

and

$$\lambda_5 = \frac{C - \left(\frac{\mu}{r^2} - \omega^2 r - \frac{V_j\beta}{m}\sin\psi\right)\lambda_1 - \left(2u\omega - \frac{V_j\beta}{m}\cos\psi\right)\lambda_2 + u\lambda_3 + \omega\lambda_4}{\beta} \quad \text{for} \quad \beta \neq 0 \tag{14}$$

REFERENCES

1. Okhotsimskiy, D. Ye., and Eneyev, T. M.: Certain Variational Problems Connected with Launching of an Artificial Earth Satellite. Symposium of Soviet Res. on Artificial Earth Satellites and Related Subjects, pt. 1, Jan. 25, 1958. (Trans. from Uspekhi Fizicheskikh Nauk, vol. 63, no. 1a, Sept. 1957, pp. 5-33.) (See also Jour. Brit. Interplanetary Soc., vol. 16, no. 5, Jan.-Feb. 1958, pp. 263-294.)

2. Irving, J. H., and Blum, E. K.: Comparative Performance of Ballistic and Low-Thrust Vehicles for Flight to Mars. Vistas in Astronautics. Vol. II. Pergamon Press, 1959, pp. 191-218.

3. Leitmann, G.: On a Class of Variational Problems in Rocket Flight. Jour. Aero/Space Sci., vol. 26, no. 9, Sept. 1959, pp. 586-591.

4. Lawden, Derek F.: Optimal Trajectories. Spec. Rep. 3, Radiation, Inc., May 1959, p. 85.

5. Melbourne, William G., and Sauer, C. G., Jr.: Optimum Thrust Programs for Power-Limited Propulsion Systems. TR 32-118, Jet Prop. Lab., C.I.T., June 15, 1961.

6. MacKay, J. S., Rossa, L. G., and Zimmerman, A. V.: Optimum Low-Acceleration Trajectories for Earth-Mars Transfer. Paper presented at IAS Conf. on Vehicle Systems Optimization, Garden City (N.Y.) Nov. 28-29, 1961.

7. Bliss, Gilbert Ames: Lectures on the Calculus of Variations. Univ. Chicago Press, 1946.

8. Moeckel, W. E.: Trajectories with Constant Tangential Thrust in Central Gravitational Fields. NASA TR R-53, 1960.